RADIO SCIENCE, Vol. 3 (New Series), No. 1, January 1968

# Exact Ray Calculations in a Quasi-Parabolic Ionosphere With No Magnetic Field

**Thomas A. Croft**

Radioscience Laboratory, Stanford University, Stanford, Calif. 94305, U.S.A.

**and**

**Harry Hoogasian**

Raytheon Company, Spencer Laboratories, Burlington, Mass. 01803, U.S.A.

(Received August 9, 1967)

The equation of the parabolic ionosphere model is modified in a manner which introduces very slight changes in the electron-density distribution. Using this new "quasi-parabolic" (or QP) model, it is possible to derive exact expressions describing radio-ray trajectories without introducing the approximations which are needed when dealing with the parabolic ionosphere, although magnetoionic effects are not included. The consequent accuracy of computed rays is useful as an aid in evaluating the accuracy of more versatile ray-calculation methods. Also, the exact ray expressions can be of direct use in calculating slight differences between rays which are nearly identical, for in this process, small inaccuracies can become magnified.

## 1. Introduction

The parabolic model of the ionosphere was introduced by Försterling and Lassen (1931), who showed that radio-ray trajectories in this model could be readily calculated if a few reasonable approximations were made. Subsequent investigators made refinements (e.g., Appleton and Beynon, 1940; Rawer, 1948) but the method has remained approximate to this day. The tractability of the ray equations has made the parabolic ionosphere very popular as a means for analysis of ionospheric radio propagation.

As implied by the name, the model is defined by the equation of a parabola in electron density versus height. In the notation which is most convenient for our purposes, the parabolic layer is

$$N_e = \begin{cases} N_m\left[1-\left(\dfrac{r-r_m}{y_m}\right)^2\right] & r_b < r < r_m + y_m \\ 0 & \text{elsewhere} \end{cases} \tag{1}$$

where $N_e$ = electron density, having maximum value $N_m$
$r$ = radial distance from earth center (height + earth radius)
$r_m$ = value of $r$ where $N_e = N_m$ ($h_m$ + earth radius)
$r_b$ = value of $r$ at the layer base = $r_m - y_m$
$y_m$ = layer semithickness.

We wish to point out that a very slight modification to the parabolic model permits the derivation of *exact* equations for ray-path parameters. This modified parabolic ionosphere will be termed the "quasi-parabolic" or, more simply, the "QP" model. The exactness of the resulting ray equations probably provides a negligible benefit in many of the more approximate applications of the

parabolic layer. However, if one wishes to investigate small differences between rays which are nearly identical, the use of the QP model will eliminate any suspicion that differences are introduced by the parabolic layer approximations. Also, a very important application for the QP model is the service it can provide as a primary standard of accuracy for testing more versatile ray-tracing methods.

The QP model was described in the literature by de Voogt (1953) in a form which bears little superficial similarity to the presentation here but which nevertheless was fundamentally the same. This original work was not widely used, apparently because of the difficulty in evaluating the expressions for the ray parameters using manual techniques. Probably for this reason, de Voogt did not publish the expressions. We believe that the QP ionospheric model will become increasingly useful because of the widespread availability of digital computers; the ray-parameter expressions described here may readily be evaluated by any computer and even by many of the small desk calculators now coming into use. Thus, in a sense, the justification for using the approximations of a parabolic ionosphere is disappearing with the advent of efficient computing machinery.

The QP layer is defined by

$$N_e=\begin{cases} N_m\left[1-\left(\frac{r-r_m}{y_m}\right)^2\left(\frac{r_b}{r}\right)^2\right]; & r_b<r<r_m\left(\frac{r_b}{r_b-y_m}\right) \\ 0 & \text{elsewhere} \end{cases} \tag{2}$$

The significant change from (1) is the addition of a multiplier, $(r_b/r)^2$. Since $r_b \approx r$ in the region of interest, the electron density versus height is nearly the same as that of a parabola having the same $r_m$ and $y_m$. The semithickness is still $y_m$, the geocentric height of the maximum is still $r_m$, and the geocentric base height is still $r_b$. The difference between this QP and a parabolic layer is the precise variation of electron density between the peak and the bottom of the layers. Figure 1 shows overlapping plots of parabolic and QP models computed and plotted by machine in order to preserve unbiased accuracy. A fine plotting pen has been used to permit the difference between layers to be seen, and even with this precaution the distinction is readily visible only when the semithickness is 200 km. This shows that the QP model is indeed very close to its parabolic predecessor. The separation between the models is more pronounced above the layer maximum, but this is not shown on figure 1 because it cannot affect the rays which will be considered here.

## 2. Calculation of Ray Parameters

It is convenient to define $F=f/f_c$, the ratio of operating frequency to critical frequency. If we neglect the geomagnetic field and collisions, then $f_c^2=80.6\ N_m$ in MKS units and the refractive index, $\mu$, is defined by

$$\mu^2=1-\frac{80.6N_e}{f^2}=1-\frac{1}{F^2}+\left(\frac{r_m-r}{F\,y_m}\right)^2\left(\frac{r_b}{r}\right)^2. \tag{3}$$

When Snell's law is applied to such a spherically symmetric system, the law of refraction assumes a special form (Bouger's rule) best expressed by noting that the product $r\mu\cos\beta$ does not vary along a single ray. Using the notation of figure 2, it is seen that $r\mu\cos\beta=r_0\cos\beta_0$. By considering the geometry of a differential ray segment and noting the symmetry about the ray apogee, the application of this law leads to integral representations of the desired ray parameters:

$D$, the distance traversed, measured along the earth's surface
$P'$, the group path (the signal transit time multiplied by $c$)
$P$, the phase path (the wavefront transit time multiplied by $c$, or the total number of wavelengths along the ray multiplied by the free-space wavelength).

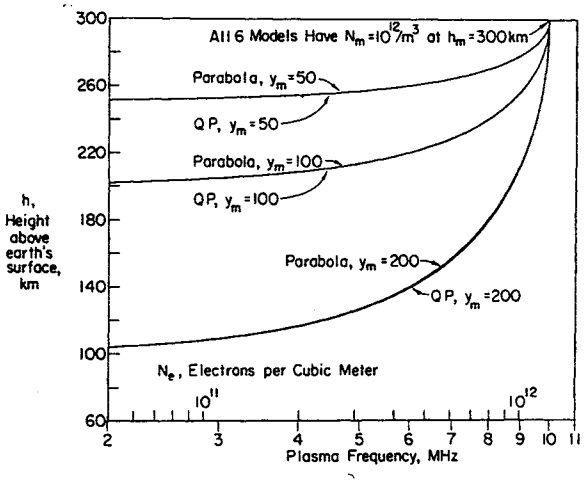


FIGURE 1. *Comparison of parabolic and quasi-parabolic models of the ionosphere.*

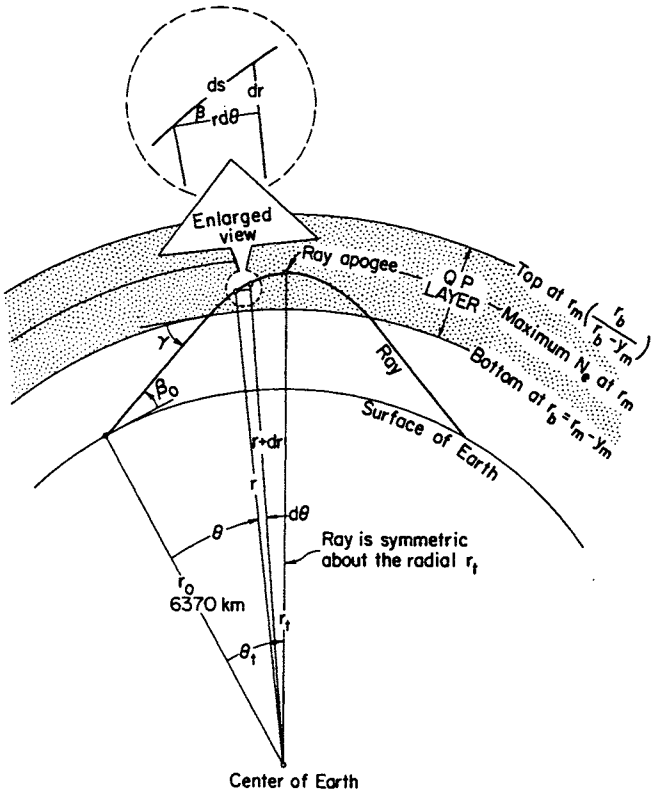


FIGURE 2. *Ray path geometry.*

$$D = 2r_0 \int_0^{\theta_t} d\theta = 2r_0 \int_{r_0}^{r_t} \frac{dr}{r \tan \beta} = 2 \int_{r_0}^{r_t} \frac{r_0^2 \cos \beta_0}{r \sqrt{r^2\mu^2 - r_0^2 \cos^2 \beta_0}} dr \tag{4a}$$

$$P' = 2 \int_0^{s_t} \frac{ds}{\mu} = 2 \int_{r_0}^{r_t} \frac{dr}{\mu \sin \beta} = 2 \int_{r_0}^{r_t} \frac{r dr}{\sqrt{r^2\mu^2 - r_0^2 \cos^2 \beta_0}} \tag{4b}$$

$$P = 2 \int_0^{s_t} \mu ds = 2 \int_{r_0}^{r_t} \frac{\mu}{\sin \beta} dr = 2 \int_{r_0}^{r_t} \frac{r\mu^2 dr}{\sqrt{r^2\mu^2 - r_0^2 \cos^2 \beta_0}} \tag{4c}$$

These three equations apply to any ionosphere concentric with the earth. However, the difficulties in evaluating the integrals in closed form limit their application to a few specific profiles such as the QP layer. In this instance, the profile has been defined in (2) as a piecewise function of altitude, so that (4a, b, c) must be separated into their free space and ionospheric parts. For the ionospheric component, the expression under the radical becomes

$$r^2\mu^2 - r_0^2 \cos^2 \beta_0 = r^2 \left(1 - \frac{1}{F^2} + \frac{r_b^2}{F^2 y_m^2}\right) - \frac{2 r_m r_b^2}{F^2 y_m^2} r + \left(\frac{r_b r_m}{F y_m}\right)^2 - r_0^2 \cos^2 \beta_0 = Ar^2 + Br + C$$

with

$$A=1-\frac{1}{F^2}+\left(\frac{r_b}{Fy_m}\right)^2$$

$$B=-\frac{2r_m r_b^2}{F^2 y_m^2}$$

$$C=\left(\frac{r_b r_m}{Fy_m}\right)^2-r_0^2\cos^2\beta_0.$$

In free space the refractive index is unity. With the foregoing substitutions, (4a, b, c) become

$$D=2r_0^2\cos\beta_0\left\{\int_{r_0}^{r_b}\frac{dr}{r\sqrt{r^2-r_0^2\cos^2\beta_0}}+\int_{r_b}^{r_t}\frac{dr}{r\sqrt{Ar^2+Br+C}}\right\} \tag{5a}$$

$$P'=2\left\{\int_{r_0}^{r_b}\frac{rdr}{\sqrt{r^2-r_0^2\cos^2\beta_0}}+\int_{r_b}^{r_t}\frac{rdr}{\sqrt{Ar^2+Br+C}}\right\} \tag{5b}$$

$$P=2\left\{\int_{r_0}^{r_b}\frac{rdr}{\sqrt{r^2-r_0^2\cos^2\beta_0}}+\int_{r_b}^{r_t}\frac{r\mu^2dr}{\sqrt{Ar^2+Br+C}}\right\}\text{with }\mu^2\text{ from (3).} \tag{5c}$$

These integrals are standard forms whose solutions are given in many tables. In carrying out the necessary algebra, it is convenient to introduce $\gamma$, the angle of the ray at the bottom of the ionosphere as shown in figure 2. The final results are:

$$D=2r_0\left\{(\gamma-\beta_0)-\frac{r_0\cos\beta_0}{2\sqrt{C}}\ln\frac{B^2-4AC}{4C\left(\sin\gamma+\frac{1}{r_b}\sqrt{C}+\frac{1}{2\sqrt{C}}B\right)^2}\right\} \tag{6a}$$

$$P'=2\left\{r_b\sin\gamma-r_0\sin\beta_0+\frac{1}{A}\left[-r_b\sin\gamma-\frac{B}{4\sqrt{A}}\ln\frac{B^2-4AC}{(2Ar_b+B+2r_b\sqrt{A}\sin\gamma)^2}\right]\right\} \tag{6b}$$

$$P=2\left\{-r_0\sin\beta_0+\frac{B}{4}\left[\frac{1}{\sqrt{A}}\ln\frac{B^2-4AC}{4\left(Ar_b+\frac{B}{2}+\sqrt{A}r_b\sin\gamma\right)^2}+\frac{r_m}{\sqrt{C}}\ln\frac{B^2-4AC}{4C\left(\sin\gamma+\frac{\sqrt{C}}{r_b}+\frac{B}{2\sqrt{C}}\right)^2}\right]\right\}. \tag{6c}$$

Some useful ancillary results for the QP layer are the following:

$Ar_t^2+Br_t+C=0$ Equation of ray apogee height

$\cos\gamma=\frac{r_0}{r_b}\cos\beta_0$ Angle of ray at bottom of ionosphere

$r_{t,\max}=-\frac{B}{2A}$ Maximum apogee height (steeper rays will penetrate the ionosphere).

## 3. Sample Calculations

A number of calculated rays are presented here in a compact graphical format; also, a few rays will be described numerically to preserve accuracy. These rays are given to provide sample answers for readers who do not wish to evaluate (6a, b, c) and also to aid in checking calculation routines designed to evaluate the equations. The present authors have independent computer

programs which evaluate $D$, $P'$, and $P$; and the answers agree within 1 part in $10^7$ for distance and group path and within 1 part in $10^6$ for phase path. The lesser accuracy on the phase path calculation arises because there is a subtraction of two numbers which are nearly equal, thereby degrading the accuracy of the result by about an order of magnitude.

Figure 3 shows a "reflectrix" family at intervals of 1 MHz, computed for a representative QP ionosphere. This format has been chosen because it simultaneously shows takeoff angle, ground distance, and virtual height. For any reflectrix point, the distance is determined by dropping a radial onto the curved base line and noting the scale provided. The virtual height is the length of this projection, a scale for which is given on the left axis. The takeoff angle is measured as an angle above the optical horizon, which is shown as a separate line. In addition, the group delay may be obtained by measuring the distance from the range-height origin to the point in question, using the group delay scale shown at the bottom of the plot. This measure is actually the length of the equivalent triangular ray and is based on a theorem of Breit and Tuve (1926) which is exact only for a flat earth-ionosphere geometry. Thus, the group delay scale is approximate while the distance, takeoff angle, and virtual height scales are accurate. This reflectrix construction was introduced by Lejay and Lepechinsky (1950), and a more recent description of it has been given by Croft (1967). Figure 3 was computed and plotted by accurate automatic techniques, but there may be some slight distortion in the reproduction.

As an aid in the checkout of computation methods, table 1 gives a few ray descriptions in numerical form. The agreement between our independent computations leads us to surmise that these numbers are correct to the last digit given but it is possible that the agreement was fortuitous.

## 4. Applications and Limitations of the Exact Equations

The accuracy of the technique given in this paper serves only as a mathematical convenience and does not represent a significant increase in the realism of the calculated rays when compared to those which may be obtained from a parabolic model. Both the parabolic and the QP ionospheres are grossly simplified representations of the real ionosphere. In particular, the rays which make only a shallow penetration into the parabolic or QP models are not much different from the rays which could be obtained by simply reflecting them off an equivalent ionospheric mirror. The geomagnetic field is ignored in both the parabolic and the QP calculations, but this is unavoidable because there is no exact ray solution known to the authors which includes the field. The fact that table 1 is good to six digits rather than four is an advantage for many purposes, but it should

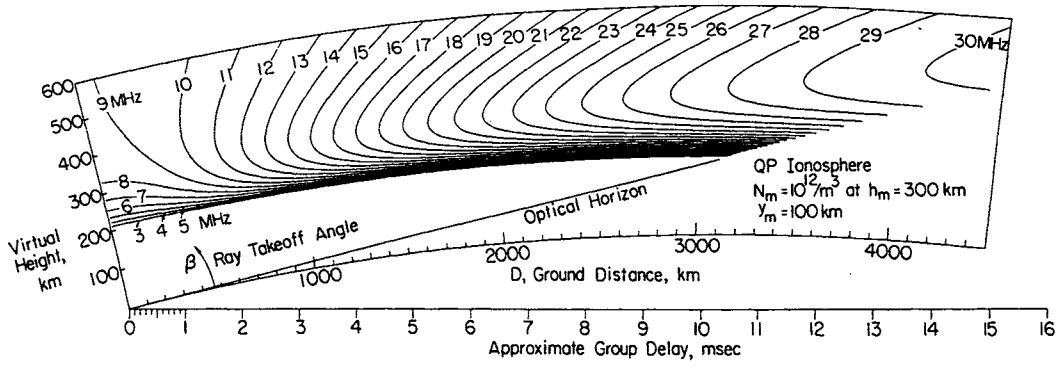


FIGURE 3. *Reflectrixes showing radio propagation in a representative QP ionosphere.*

From any point on a reflectrix for a selected frequency, drop a radial to the curved baseline to find ground distance of ray. The length of the radial is the virtual height, using the scale given on the left. From the same point draw a line to the distance-height origin; the angle between this line and the optical horizon is the ray takeoff angle. Finally, the length of the line is (approximately) the ray group delay, using the lower scale.

TABLE 1. *Computed Rays in a QP layer;* $N_m = 10^{12}/m^3$, $h_m = 300$ *km* $(= r_m - r_0)$, $y_m = 100$ *km*

| Radio frequency, MHz | Takeoff angle, degrees | Ground distance, km | Group path, km | Phase path, km |
|---|---|---|---|---|
| 20 | 0 | 3428.874 | 3513.514 | 3500.35 |
| | 4 | 2673.309 | 2760.273 | 2745.35 |
| | 8 | 2161.267 | 2256.988 | 2236.08 |
| | 12 | 1842.605 | 1955.747 | 1922.15 |
| | 16 | 1685.174 | 1829.296 | 1769.19 |
| | 20 | 1841.034 | 2065.866 | 1916.15 |
| 29 | 0 | 4128.680 | 4268.531 | 4210.13 |
| | 1 | 3923.094 | 4063.916 | 4004.56 |
| | 2 | 3752.455 | 3896.388 | 3833.98 |
| | 3 | 3622.093 | 3771.912 | 3703.74 |
| | 4 | 3546.615 | 3706.676 | 3628.40 |
| | 5 | 3577.037 | 3756.917 | 3658.70 |

be realized that the second (or even the first) digit may be wrong if the rays are used as a substitute for those which occur in the real ionosphere.

When these results are used to test versatile ray-tracing programs, one must still be cautious about interpreting the significance of high accuracy. For example, almost all ray-tracing programs ignore the fact the the earth's radius varies by 20 km depending on observer location. (What, then, is a "nontilted ionosphere?") Similarly, it is known that the index of refraction exceeds unity by a significant amount in the lowest 20 km of altitude, and that the consequent bending (usually neglected) will increase the ground range of low-angle rays from 1 to 3 percent. Perhaps the greatest source of error in all ray calculations is the uncertainty in the specific ionospheric models which must be used.

The extreme accuracy which can be obtained by numerical ray tracing does serve a useful purpose when comparisons must be made between two rays which are nearly identical. Such comparison often involves the calculation of a small difference between two large numbers, and in this circumstance the fourth, fifth, or sixth digit may be crucial.

---

The part of this work performed at Raytheon was supported by the Propagation Sciences Laboratory of the Air Force Cambridge Research Laboratories under contract AF19(604)–5230. The part conducted at Stanford was supported by the Advanced Research Projects Agency under contract Nonr–225(64).

## 5. References

Appleton, E. V., and W. J. G. Beynon (1940), The application of ionospheric data to radio-communication problems: Pt. 1. Proc. Phys. Soc. London **52**, No. 202, 518–533.

Breit, G., and M. A. Tuve (1926), A test of the existence of the conducting layer, Phys. Rev. **28**, No. 3, 554–573.

Croft, T. A. (1967), HF radio focusing caused by the electron distribution between ionospheric layers, J. Geophys. Res. **72**, No. 9, 2343–2355.

de Voogt, A. H. (1953), The calculation of the path of a radio-ray in a given ionosphere, Proc. IRE **41**, No. 9, 1183–1186.

Försterling, V. K., and H. Lassen (1931), Die Ionisation der Atmosphäre und die Ausbreitung der kurzen elektrischen Wellen (10–100 m) über die Erde. III, Zeitschrift fur technische Physik, **12**, 502–527.

Lejay, P., and D. Lepechinsky (1950), Field intensity at the receiver as a function of distance, Nature **165**, No. 4191, 306–307.

Rawer, K. (1948), Optique Géométrique De L'Ionosphère, Rev. Sci. Paris, No. 3298, 585–600 (4 Rue Pomereu, Paris).

(Paper 3–1–330)